

A Kerr Polarization Controller

N. Moroney^{1,2}, L. Del Bino¹, S. Zhang¹, M. T. M. Woodley^{1,2,4}, L. Hill⁵, T. Wildi⁶,
V. J. Wittwer⁷, T. Südmeyer⁷, G.-L. Oppo⁵, M. R. Vanner², V. Brasch⁸, T. Herr⁶, and
P. Del'Haye^{1,9,*}

¹Max Planck Institute for the Science of Light, 91058 Erlangen, Germany

²QOLS, Blackett Laboratory, Imperial College London, SW7 2AZ, United Kingdom

⁴SUPA and Department of Physics, Heriot-Watt, Edinburgh EH14 4AS, United Kingdom

⁵SUPA and Department of Physics, University of Strathclyde, Glasgow G4 0NG, Scotland

⁶Center for Free-Electron Laser Science (CFEL), Deutsches Elektronen-Synchrotron (DESY), Hamburg, Germany

⁷Laboratoire Temps-Fréquence, Université de Neuchâtel, CH-2000 Neuchâtel, Switzerland

⁸Swiss Center for Electronics and Microtechnology (CSEM), Time and Frequency, Neuchâtel, Switzerland

⁹Friedrich Alexander University Erlangen-Nuremberg, Germany

*Corresponding author: pascal.delhaye@mpl.mpg.de

ABSTRACT

Kerr-effect-induced changes of the polarization state of light are well known in pulsed laser systems. An example is nonlinear polarization rotation, which is critical to the operation of many types of mode-locked lasers. Here, we demonstrate that the Kerr effect in a high-finesse Fabry-Pérot resonator can be utilized to control the polarization of a continuous wave laser. It is shown that a linearly-polarized input field is converted into a left- or right-circularly-polarized field, controlled via the optical power. The observations are explained by Kerr-nonlinearity induced symmetry breaking, which splits the resonance frequencies of degenerate modes with opposite polarization handedness in an otherwise symmetric resonator. The all-optical polarization control is demonstrated at threshold powers down to 7 mW. The physical principle of such Kerr effect-based polarization controllers is generic to high-Q Kerr-nonlinear resonators and could also be implemented in photonic integrated circuits. Beyond polarization control, the spontaneous symmetry breaking of polarization states could be used for polarization filters or highly sensitive polarization sensors when operated close to the symmetry-breaking point.

1 Introduction

Spontaneous symmetry breaking is an important concept in fundamental physics, describing the origins of bosonic mass via the Higgs mechanism¹, superconductivity², and the phases of matter³. Spontaneous symmetry breaking is characterized by a system whose Lagrangian and initial state are symmetric (invariant under some transformation), but whose lowest-energy states to which the system evolves do not share such a symmetry.

Nonlinear optical interactions and in particular the Kerr effect can also exhibit spontaneous symmetry breaking. An example is time-reversal symmetry breaking in a pulse-pumped ring cavity^{4,5}. In addition, the Kerr interaction plays an important role in the interaction of soliton frequency combs in microresonators⁶⁻¹⁰. In the continuous wave regime, spontaneous symmetry breaking has been observed¹¹⁻¹³ between counter-propagating light in microresonators with high optical quality factors. In addition, recent work has shown polarization symmetry breaking of optical pulses in fiber ring resonators with residual birefringence¹⁴⁻¹⁸.

Here, we experimentally demonstrate that Kerr-nonlinearity mediated symmetry breaking can be observed for the polarization states of continuous wave light in geometrically linear Fabry-Pérot-type cavities. This symmetry breaking is demonstrated for linearly polarized input light that is sent into a high Finesse fiber cavity. At low powers this system maintains symmetry such that the polarization of the cavity field matches that of the input. At a measured threshold power of 7 mW, spontaneous symmetry breaking of the resonator modes splits up the linear polarized light into left and right polarized light, with one handedness being transmitted and the other one reflected. We further demonstrate that the output polarization can be optically controlled by using a resonator with slight asymmetries due to birefringence. This enables us to continuously change the output polarization state from linear to elliptical and close to circular polarization. Together with an additional polarizer, the Kerr polarization symmetry breaking can be used to generate an orthogonal polarization component with respect to the linear polarized input light. This could find applications in all-optical polarization controllers for photonic circuits that require fast response times beyond thermally or mechanically actuated polarization controllers¹⁹⁻²¹. In addition, this type of polarization controller does not rely on electro-optical effects, which reduces fabrication complexity and eliminates the need for electrical connections.

The polarization interactions discussed here are mathematically analogous to the Kerr interaction between counter-propagating light^{11,12,22,23}. Thus, this effect can be similarly used for all-optical information processing and storage of information^{24–28}. Integration of this system on-chip would also give enhanced sensing of polarization effects beyond shot noise limitations.

2 Polarization symmetry breaking principle

Nonlinear interactions of light are extremely weak and are normally only appreciable in high-power systems, or those in which the intensity is resonantly enhanced. The advent of high-Q ring resonators²⁹ and Fabry-Pérot (FP) cavities³⁰ has led to extensive research in nonlinear optics at low powers and small footprints, promising application in photonic integrated circuits³¹.

The evolution of the electric field inside a resonator consisting of a nonlinear $\chi^{(3)}$ Kerr medium is given by Eq. (1), a modified version of the Lugiato-Lefever Equation³², which is normalized to dimensionless quantities, ignores dispersive and fast-time effects, and is extended to include coupled polarization effects (See Appendix A)^{22,33,34}:

$$\frac{dE_{\pm}}{dt} = \tilde{E}_{\pm} - E_{\pm} + i\delta E_{\pm} - i(|E_{\pm}|^2 + 2|E_{\mp}|^2)E_{\pm} \quad (1)$$

in which the subscript + (–) denotes the right- (left-) handed circular polarization, the first term (\tilde{E}_{\pm}) represents the input fields that are sent into the cavity, the second term ($-E_{\pm}$) represents losses inside the cavity, the third term ($i\delta E_{\pm}$) represents the field-cavity detuning and the final term ($-i(|E_{\pm}|^2 + 2|E_{\mp}|^2)E_{\pm}$) represents the Kerr effect.

The final two terms of Eq. (1) are of the same form and can be taken together as an effective cavity detuning. This follows from the physical manifestation of the Kerr nonlinearity in this system as an intensity-dependent refractive index, in which the effective refractive index that a beam experiences is dependent on its own intensity via self-phase modulation (SPM), and the intensity of the cross-polarized beam via cross-phase modulation (XPM). When the Kerr effect is a result of non-resonant electronic response, as in our system, the effect of XPM is twice that of SPM, leading to the factor of 2 in Eq. (1).

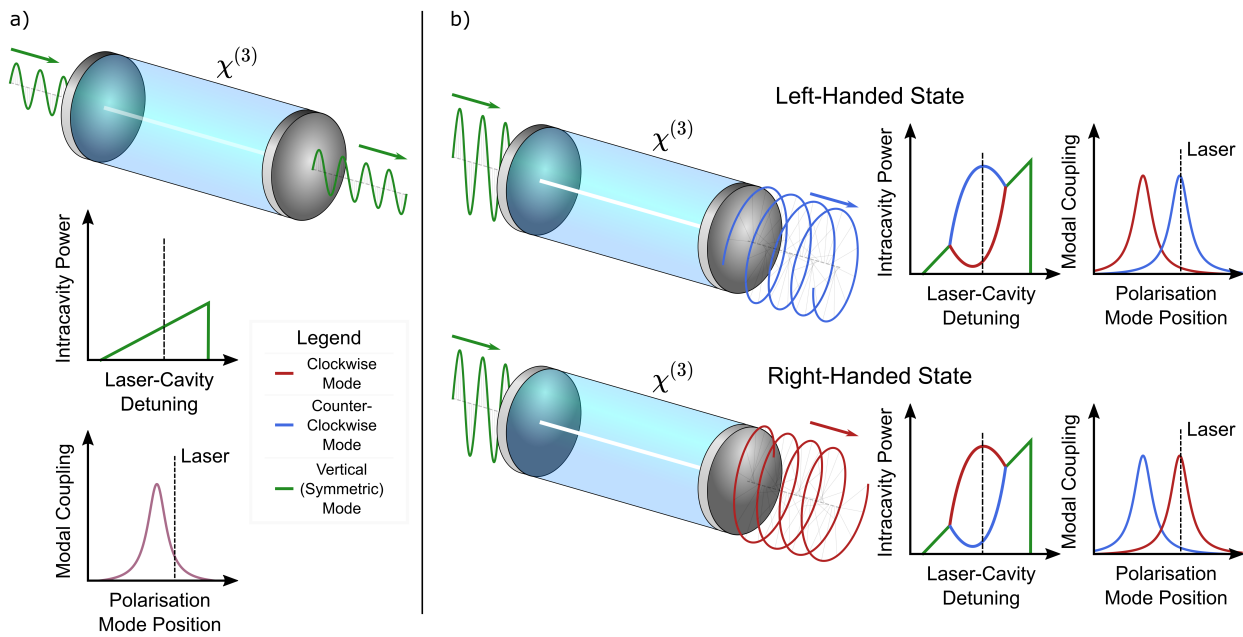


Fig. 1 | Kerr interaction of the polarization modes of light. Linearly polarized light enters a nonlinear high-Q Fabry-Pérot cavity with degenerate polarization modes. a) Below threshold power, the resonator equally supports all polarization states and the output polarization matches the input. b) The linearly polarized input light can be described as a superposition of left- and right-circular polarized light. Above a threshold power exists a regime in which the resonator cannot simultaneously support both left- and right-circular polarization modes. This leads to a spontaneous symmetry breaking in which the output develops an angular momentum with random handedness, even though the input light is linearly polarized with zero angular momentum (momentum is conserved with the reflection of the opposite handed light). The plots on the right in panel b) show the intracavity power and resonance frequencies of the symmetry broken states.

The steady-state intracavity powers can be found from Eq. (1):

$$|E_{\pm}|^2 = \frac{|\tilde{E}_{\pm}|^2}{1 + (|E_{\pm}|^2 + 2|E_{\mp}|^2 - \delta)^2} \quad (2)$$

which can be understood as a tilted Lorentzian response with nonlinear effective detunings $\delta_{\text{eff},\pm} = \delta - |E_{\pm}|^2 - 2|E_{\mp}|^2$.

The symmetry of Eq. (2) can be seen by interchanging the \pm indices, provided that the inputs to both modes are equal ($\tilde{E}_+ = \tilde{E}_-$ i.e. a linearly polarized input). Fig. 1a) shows the expected response of this system to a linearly polarized input that is frequency-scanned across a resonance without breaking of the symmetry; Kerr and thermal nonlinearities give the resonance a triangular shape³⁵, and the symmetry in the system ensures that both cross-polarized components of the input couple equally, preserving the polarization of the input. However, above some threshold power, and for a range of detunings, this symmetric state becomes unstable due to the differing magnitudes of SPM and XPM²². Under these conditions, any small difference in intensity between the two modes is amplified because the stronger mode drives the weaker mode further out of resonance via XPM. Fig. 1b) shows how random noise leads the system to spontaneously adopt a handedness, with one mode dominating over the other.

It appears as if this system has broken conservation of angular momentum, since the input has no angular momentum but the cavity field has a handedness. This is not the case, instead the linear input has been broken into its constituent components of opposite angular momenta, with one dominating the coupling into the cavity. The opposite handedness is reflected from, rather than transmitted through, the cavity, and thus conserves angular momentum.

This process can also be viewed as a partial conversion of the linear polarized input light into an orthogonal polarization state. The input to the cavity is vertically polarized, so has no horizontal component, however the resulting cavity/output fields are elliptical (due to the partial rejection of one circular polarization), which now must have a horizontal component that is $\pm\pi$ out of phase with the vertical component. Accordingly, the process can either be characterised by the difference in the output intensities in the circular basis, or by the generation of light in the horizontal basis.

3 Experimental setup for spontaneous polarization symmetry breaking

Figure 2 shows a schematic for the experimental setup. The cavity for this work is made from a 2-meter-long single-mode silica fiber, connected at both ends to highly reflective dielectric Bragg mirrors that are coated onto fiber ends³⁶. The mirrors have a reflectivity $> 99\%$ at 1550 nm. Together, they form a high-finesse cavity ($F \approx 140$) with very narrow linewidths ($\delta\nu \approx 0.40$ MHz, $Q \approx 4.9 \times 10^8$). Even though the finesse is already high, these parameters could be further improved by directly depositing the mirrors on both ends of a fiber to form a cavity, minimizing the losses at the connector.

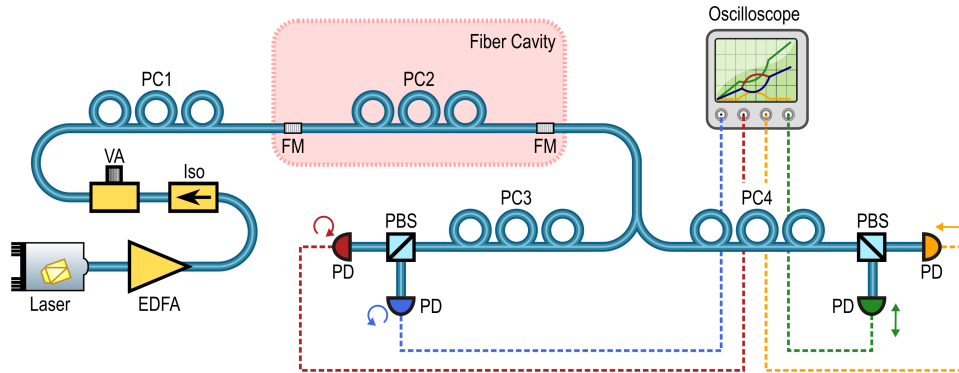


Fig. 2 | Experimental Schematic. A high-finesse Fabry-Pérot fiber cavity is realized by connecting an optical fiber on both ends to fibers with dielectric Bragg mirror stacks (fiber mirror, FM). To attain degenerate polarization modes, a polarization controller (PC2) is placed within the cavity, which is used to cancel any birefringence in the fiber and mirrors. Light is sent into the cavity from a tunable diode laser via an erbium-doped fiber amplifier (EDFA) with an isolator (Iso) to prevent back reflections. A variable attenuator (VA) is then used to control the power of the input light and its polarization is set by polarization controller PC1. The output of the cavity is split by a 50:50 fiber coupler and each branch is directed to photo-diodes (PD) via PC3,4 and polarization beam splitters (PBS). These final PCs are used to map the cavity's polarization states to the PBS such that the PDs each monitor a distinct polarization mode of the resonator.

Polarization symmetry breaking requires the splitting of the resonances to be dominated by the Kerr effect; the splitting due to birefringence (a manifestation of linear coupling between polarization modes) should be minimal. In principle this resonator should show degenerate polarization modes, however asymmetries in the mirror deposition and stresses in the fiber lead to some slight amount of birefringence which cannot be neglected due to the narrow linewidth of this resonator. To observe symmetry breaking, it was found experimentally that this linear resonance splitting must be significantly below 5% of the cavity linewidth which gives a strict requirement on the birefringence of $\delta n/n < 0.05/Q \lesssim 1 \times 10^{-10}$. The residual birefringence could be eliminated with more careful waveguide design or by using spun fibers. In this work we use an intracavity polarization controller to eliminate the residual birefringence.

In the experiment, light from a tunable diode laser is amplified by an erbium-doped fiber amplifier (EDFA), before being sent through an isolator to minimize unwanted effects from back reflections of the fiber cavity. The output polarization of the EDFA changes with power, so the power input to the cavity is instead controlled using a variable attenuator which maintains polarization across the required power range. Finally, the input polarization is set to linear by a polarization controller (PC1) before entering the cavity. This polarization state is henceforth defined to be the vertical polarization direction.

Light then enters the cavity and builds up in intensity, with some part exiting through the output port. The output signal is then split and each branch is sent to a photodiode via a polarization controller and polarization beam splitter (PBS). The polarization controllers are set to map the cavity polarization modes to the PBS basis, with one branch monitoring the opposite circular polarizations and the other monitoring the vertical and horizontal polarizations. The signals from the photodiodes can then be used for real-time monitoring of the cavity polarization state when the laser frequency is swept across a resonance.

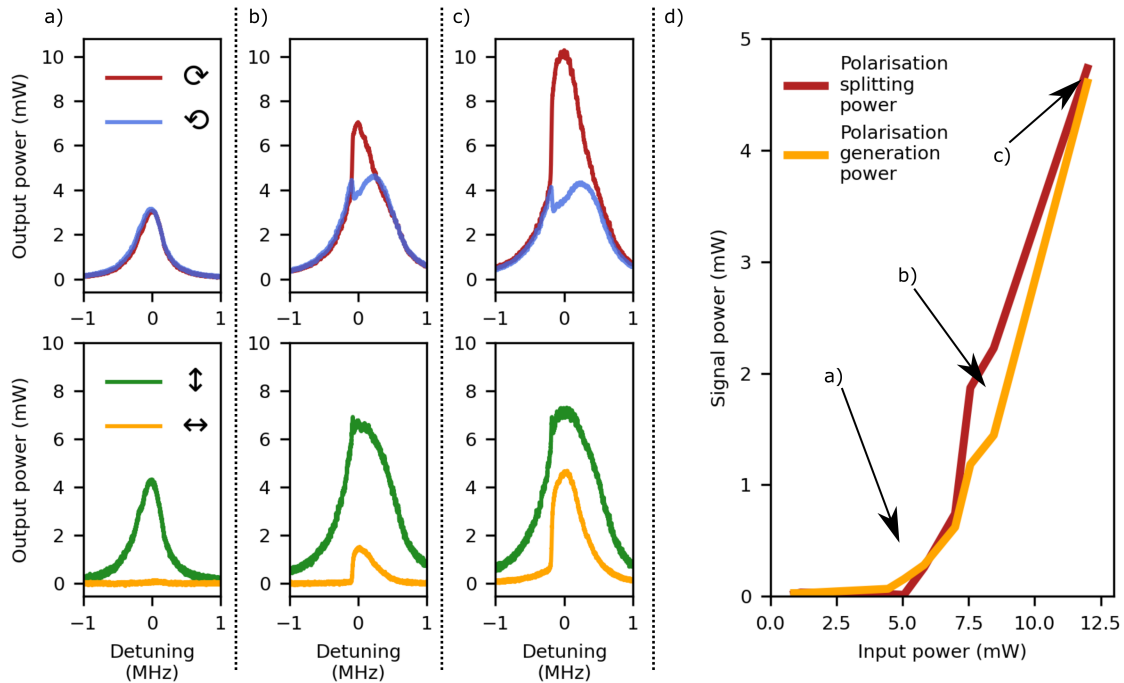


Fig. 3 | Measurement of Spontaneous Polarization Symmetry Breaking a) At low powers, both the right- (red) and left-handed (blue) polarization states couple equally into the cavity. This corresponds to the output light always having vertical polarization (green), with no horizontal (yellow) component. b) Above threshold, spontaneous symmetry breaking changes the relative optical power in the different polarization modes in a range of cavity detunings. In this regime, there has been the spontaneous generation of horizontally polarized light, and a reduced amount of the vertical polarization. c) The symmetry breaking increases at higher input powers. d) Threshold behavior for the polarization symmetry breaking. The red curve shows the maximum power difference between left- and right-circular light for different input powers. The yellow curve shows the power of the generated horizontally polarized light.

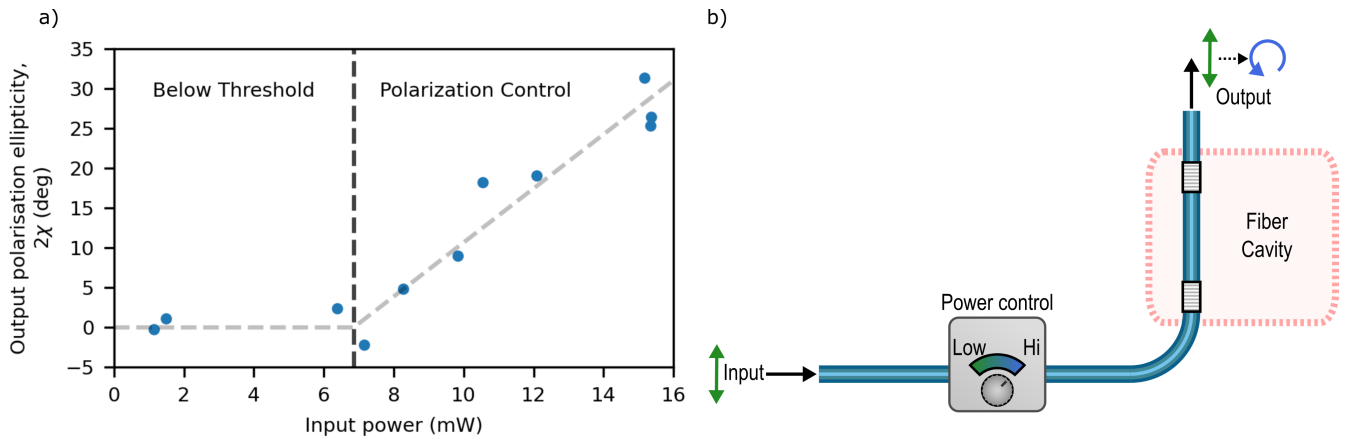


Fig. 4 | Polarization control using the Kerr effect a) Experimental demonstration of the control of the output field's ellipticity, given by the Stokes parameter χ , for different input powers. The output light remains linearly polarized ($\chi = 0$) for powers below threshold after which it becomes increasingly circular with increasing input power. b) Concept of a Kerr polarization controller. Linearly polarized light is input into a cavity such that the output polarization can be controlled by modifying the input intensity. The cavity must be slightly biased towards one circular polarization, forcing the output to have the intended handedness rather than spontaneously developing a random handedness.

4 Results

The transmission through the cavity for polarization states at different input powers is shown in Fig. 3. At low powers, the linear input polarization couples equally into the left and right circular polarization modes of the cavity as would be expected for a system without birefringence. Correspondingly, this means that the output polarization matches the input for any cavity detuning; taking the input polarization to be vertical, there is no horizontal component to the output.

Above a threshold input power of 7 mW, spontaneous symmetry breaking is observed. This is exhibited by a difference in the output powers of opposite circular polarizations. In addition, we observe the sudden spontaneous generation of horizontally polarized light, which is the manifestation of the same phenomenon in a different basis. Larger input powers lead to a greater power splitting, consistent with the power dependence of the Kerr effect.

In principle, the direction of the symmetry breaking i.e. the handedness of the output light should be random for every sweep of the laser through the cavity resonance. In practice, a dominant direction was seen due to residual cavity birefringence and imperfect input polarization. A small handedness in the input light leads to a preferred symmetry breaking direction, which can be used for highly sensitive polarization sensors. In addition, residual birefringence allows one mode to couple in before the other during the laser sweep, making it dominant (this effect would then be dependent on the direction of the laser frequency sweep).

Intentionally biasing the resonator with a dominant circular polarization allows for the realization of a Kerr polarization controller. Fig. 4a shows how the output field's Stokes parameter χ - a measure of the ellipticity of the polarization - can be controlled using the input power. Below a threshold power, the output light remains linearly polarized ($\chi = 0$), and becomes increasingly circularly polarized ($\chi \rightarrow 90^\circ$) with increasing input power. Accordingly, a suitably biased cavity can be used to form a polarization controller (Fig. 4b) for which the output polarization is dependent on the input intensity.

5 Conclusion

We demonstrate the spontaneous symmetry breaking of the polarization state of continuous-wave light in Fabry-Pérot-type optical resonators. Above a threshold power of 7 mW, the Kerr effect spontaneously splits up linear polarized input light into left- and right-circular polarized light, with only one of the two polarization directions being transmitted, allowing for all-optical control of the polarization state of the output light. This effect is applicable to any high-Q Kerr resonator with sufficiently small birefringence and could be used in mm-scale fiber cavities or chip-integrated microresonators. As such, the polarization symmetry breaking offers the possibility to be used in a number of applications, most evidently as nonlinear polarization filters but also as all-optical polarization controllers and enhanced polarization sensors. A number of these devices could be cascaded to map an arbitrary input polarization to any output state based on the power and detuning of the input. Such all-optical polarization control could also be of interest for applications in environments in which electronic polarization control is not feasible or not practical. As a sensor, the bifurcation at the symmetry breaking point gives a strong sensitivity

of the system to the input polarization state which could be beneficial for e.g. optical neural networks, quantum information processing, and lab-on-chip systems.

6 Acknowledgements

This work was supported by the European Union's H2020 ERC Starting Grant "CounterLight" 756966, the H2020 Marie Skłodowska-Curie COFUND "Multiply" 713694, the Marie Curie Innovative Training Network "Microcombs" 812818, the Max Planck Society, and the Engineering and Physical Sciences Research Council (EPSRC) via the CDTs for Applied Photonics and Quantum Systems Engineering.

7 Author Contributions

N.M. and P.D. conceived and designed the experiments. N.M., L.D. and S.Z. performed the measurements. N.M., L.D.B., S.Z., M.T.M.W, G.O. and P.D.H. analyzed the results. T.W., V.J.W., T.S., V.B, and T.H. fabricated and characterized the fiber mirrors. All co-authors contributed to the manuscript.

8 Data Availability

The data that support the plots within this paper and other findings of this study are available upon reasonable request.

9 Competing interests

The authors declare no competing interests.

References

1. Strocchi, F. Spontaneous symmetry breaking in local gauge quantum field theory; the Higgs mechanism. *Comm. Math. Phys.* **56**, 57–78 (1977).
2. Sinha, D. & Amaratunga, G. A. J. Spontaneous symmetry breaking. In *Explicit Symmetry Breaking in Electrodynamical Systems and Electromagnetic Radiation* (IOP Publishing, 2016).
3. Sadler, L. E., Higbie, J. M., Leslie, S. R., Vengalattore, M. & Stamper-Kurn, D. M. Spontaneous symmetry breaking in a quenched ferromagnetic spinor Bose-Einstein condensate. *Nature* **443**, 312–315 (2006).
4. Xu, Y. & Coen, S. Experimental observation of the spontaneous breaking of the time-reversal symmetry in a synchronously pumped passive Kerr resonator. *Opt. Lett.* **39**, 3492 (2014).
5. Copie, F. *et al.* Interplay of Polarization and Time-Reversal Symmetry Breaking in Synchronously Pumped Ring Resonators. *Phys. Rev. Lett.* **122**, 013905 (2019).
6. Yang, Q. F., Yi, X., Yang, K. Y. & Vahala, K. Counter-propagating solitons in microresonators. *Nat. Photonics* **11**, 560–564 (2017).
7. Bao, C. *et al.* Orthogonally polarized frequency comb generation from a Kerr comb via cross-phase modulation. *Opt. Lett.* **44**, 1472 (2019).
8. Lucas, E. *et al.* Spatial multiplexing of soliton microcombs. *Nat. Photonics* **12**, 699–705 (2018).
9. Joshi, C. *et al.* Counter-rotating cavity solitons in a silicon nitride microresonator. *Opt. Lett.* **43**, 547–550 (2018).
10. Zhang, S., Silver, J. M., Bi, T. & Del'Haye, P. Spectral extension and synchronization of microcombs in a single microresonator. *Nat. Commun.* **11**, 1–7 (2020).
11. Del Bino, L., Silver, J. M., Stebbings, S. L. & Del'Haye, P. Symmetry Breaking of Counter-Propagating Light in a Nonlinear Resonator. *Sci. Rep.* **7**, 1–6 (2017).
12. Cao, Q. T. *et al.* Experimental Demonstration of Spontaneous Chirality in a Nonlinear Microresonator. *Phys. Rev. Lett.* **118**, 033901 (2017).
13. Woodley, M. T. *et al.* Universal symmetry-breaking dynamics for the Kerr interaction of counterpropagating light in dielectric ring resonators. *Phys. Rev. A* **98**, 053863 (2018).
14. Garbin, B. *et al.* Dissipative Polarization Domain Walls in a Passive Coherently Driven Kerr Resonator. *Phys. Rev. Lett.* **126**, 023904 (2021).
15. Fatome, J. *et al.* Polarization modulation instability in a nonlinear fiber Kerr resonator. *Opt. Lett.* **45**, 5069–5072 (2020).

16. Garbin, B. *et al.* Asymmetric balance in symmetry breaking. *Phys. Rev. Res.* **2**, 023244–023256 (2020).
17. Xu, G. *et al.* Spontaneous symmetry breaking of dissipative optical solitons in a two-component Kerr resonator. *arXiv preprint arXiv:2008.13776* (2020).
18. Hill, L. *et al.* Breathing dynamics of symmetry-broken polarized temporal cavity solitons in Kerr ring resonators. In *OSA Advanced Photonics Congress (AP) 2020 (IPR, NP, NOMA, Networks, PVLED, PSC, SPPCom, SOF) (2020)*, paper NpTu1D.3, NpTu1D.3 (The Optical Society, 2020).
19. Velha, P. *et al.* Wide-band polarization controller for Si photonic integrated circuits. *Opt. Lett.* **41**, 5656 (2016).
20. Sarmiento-Merenguel, J. D. *et al.* Demonstration of integrated polarization control with a 40 dB range in extinction ratio. *Optica* **2**, 1019–1023 (2015).
21. Xu, Q., Chen, L., Wood, M. G., Sun, P. & Reano, R. M. Electrically tunable optical polarization rotation on a silicon chip using Berry's phase. *Nat. Commun.* **5**, 1–6 (2014).
22. Hill, L., Oppo, G.-L., Woodley, M. T. M. & Del'Haye, P. Effects of self- and cross-phase modulation on the spontaneous symmetry breaking of light in ring resonators. *Phys. Rev. A* **101**, 13823 (2020).
23. Woodley, M. T., Hill, L., Del Bino, L., Oppo, G. L. & Del'Haye, P. Self-Switching Kerr Oscillations of Counterpropagating Light in Microresonators. *Phys. Rev. Lett.* **126**, 043901 (2021).
24. Moroney, N. *et al.* Logic Gates Based on Interaction of Counterpropagating Light in Microresonators. *J. Light. Technol.* **38**, 1414–1419 (2020).
25. Bino, L. D. D., Moroney, N. & Del'Haye, P. Optical memories and switching dynamics of counterpropagating light states in microresonators. *Opt. Express* **29**, 2193 (2021).
26. Cheng, Q., Bahadori, M., Glick, M., Rumley, S. & Bergman, K. Recent advances in optical technologies for data centers: a review. *Optica* **5**, 1354 (2018).
27. Sasikala, V. & Chitra, K. All optical switching and associated technologies: a review. *J. Opt. (India)* **47**, 307–317 (2018).
28. Wang, J. & Long, Y. On-chip silicon photonic signaling and processing: a review (2018).
29. Liu, J. *et al.* Ultralow-power chip-based soliton microcombs for photonic integration. *Optica* **5**, 1347–1353 (2018).
30. Brasch, V., Obrzud, E., Lecomte, S. & Herr, T. Nonlinear filtering of an optical pulse train using dissipative Kerr solitons. *Optica* **6**, 1386 (2019).
31. Ge, L., Feng, L. & Schwefel, H. G. L. Optical microcavities: new understandings and developments. *Photon. Res.* **5**, OM1–OM3 (2017).
32. Lugiato, L. A. & Lefever, R. Spatial Dissipative Structures in Passive Optical Systems. *Phys. Rev. Lett.* **58**, 2209—2211 (1987).
33. Geddes, J. B., Moloney, J. V., Wright, E. M. & Firth, W. J. Polarisation patterns in a nonlinear cavity. *Opt. Commun.* **111**, 623–631 (1994).
34. Cole, D. C., Gatti, A., Papp, S. B., Prati, F. & Lugiato, L. Theory of Kerr frequency combs in Fabry-Perot resonators. *Phys. Rev. A* **98**, 13831 (2018).
35. Carmon, T., Yang, L. & Vahala, K. J. Dynamical thermal behavior and thermal self-stability of microcavities. *Opt. Express* **12**, 4742–4750 (2005).
36. Obrzud, E., Lecomte, S. & Herr, T. Temporal solitons in microresonators driven by optical pulses. *Nat. Photonics* **11**, 600–607 (2017).
37. Boyd, R. W. *Nonlinear Optics*. Nonlinear Optics Series (Elsevier Science, 2020), 4 edn.

A Appendix: Cross-phase modulation between polarization modes of light

The evolution of the electric field (\vec{E}) in a nonlinear resonator is given by the Lugiato-Lefever equation³², which is here generalised to allow for field polarization³³, and dispersive effects are neglected (we assume a uniform, slowly evolving cavity field):

$$\frac{\partial \vec{E}}{\partial t} = -(1 + i\delta)\vec{E} + \tilde{\vec{E}} + i \left(A \left(\vec{E} \cdot \vec{E}^* \right) \vec{E} + \frac{B}{2} \left(\vec{E} \cdot \vec{E} \right) \vec{E}^* \right) \quad (3)$$

where \vec{E} is the input field, δ is the cavity detuning parameter. The nonlinear term, $A \left(\vec{E} \cdot \vec{E}^* \right) \vec{E} + \frac{B}{2} \left(\vec{E} \cdot \vec{E} \right) \vec{E}^*$ can be simplified as $A = B$ for nonresonant electronic response (the source of nonlinearity in silica)^{5,37}.

The electric field can be split two linear components: \vec{x}, \vec{y} :

$$\vec{E} = E_x \vec{x} + E_y \vec{y} \quad (4)$$

for which Eq. (3) becomes:

$$\frac{\partial E_{x,y}}{\partial t} = -(1 + i\delta) E_{x,y} + \tilde{E}_{x,y} + iA \left([|E_x|^2 + |E_y|^2] E_{x,y} + \frac{1}{2} [E_x^2 + E_y^2] E_{x,y}^* \right) \quad (5)$$

The nonlinear term in Eq. (5) shows equal amounts of self- and cross-phase modulation along with a phase-dependent term. The equal effects of self- and cross-phase modulation ensure that it is not possible to break symmetry in this basis.

The circular basis is defined as:

$$E_{\pm} = \frac{E_x \pm iE_y}{\sqrt{2}} \quad (6)$$

Such that:

$$\frac{\partial E_{\pm}}{\partial t} = \frac{1}{\sqrt{2}} \left(\frac{\partial E_x}{\partial t} \pm i \frac{\partial E_y}{\partial t} \right) \quad (7)$$

which on insertion of Eq. (5) becomes:

$$\begin{aligned} \frac{\partial E_{\pm}}{\partial t} &= -(1 + i\delta) E_{\pm} + \tilde{E}_{\pm} + iA \left([|E_x|^2 + |E_y|^2] E_{\pm} + \frac{1}{2} [E_x^2 + E_y^2] E_{\mp}^* \right) \\ &= -(1 + i\delta) E_{\pm} + \tilde{E}_{\pm} + iA \left([|E_{\pm}|^2 + |E_{\mp}|^2] E_{\pm} + E_{\pm} E_{\mp} E_{\mp}^* \right) \\ &= -(1 + i\delta) E_{\pm} + \tilde{E}_{\pm} + iA E_{\pm} (|E_{\pm}|^2 + 2|E_{\mp}|^2) \end{aligned} \quad (8)$$

in which cross-phase modulation now has twice the strength of self-phase modulation and so symmetry breaking is possible²².

The circular polarization basis is the only one without the phase terms of Eq. (5) and thus is the natural basis in which to describe the interactions. Accordingly, the input must be linearly polarized (i.e. an equal pumping of both circular directions), and the symmetry broken state will spontaneously tend to one of the circular handed states.

At steady state, Eq. (8) is zero such that:

$$\begin{aligned} 0 &= -(1 + i\delta) E_{\pm} + \tilde{E}_{\pm} + iA E_{\pm} (|E_{\pm}|^2 + 2|E_{\mp}|^2) \\ E_{\pm} &= \frac{\tilde{E}_{\pm}}{1 + i(\delta - A(|E_{\pm}|^2 + 2|E_{\mp}|^2))} \\ |E_{\pm}|^2 &= \frac{|\tilde{E}_{\pm}|^2}{1 + (\delta - A(|E_{\pm}|^2 + 2|E_{\mp}|^2))^2} \end{aligned} \quad (9)$$

which after normalizing all intensities by A gives Eq. (2).

The Stokes parameter which defines the ellipticity of light, 2χ , can then be calculated from:

$$2\chi = \arctan \left(\frac{1}{2} \left(\frac{|E_+|}{|E_-|} - \frac{|E_-|}{|E_+|} \right) \right) \quad (10)$$

in which $2\chi = 0$ for linearly polarized light i.e. $|E_+| = |E_-|$, and $2\chi = \frac{\pi}{2} \left(-\frac{\pi}{2} \right)$ for right- (left-) handed circular polarized light i.e. $|E_-| = 0 \left(|E_+| = 0 \right)$.